Inhibited Light Propagation and Broadband Reflection in Photonic Air-Sphere Crystals

Michiel S. Thijssen,[1] Rudolf Sprik,[1] Judith E. G. J. Wijnhoven,[1] Mischa Megens,[1] T. Narayanan,[2] Ad Lagendijk,[1] and Willem L. Vos[1,*]

[1]*Van der Waals-Zeeman Instituut, Universiteit van Amsterdam, 1018 XE Amsterdam, The Netherlands*
[2]*ESRF, BP 220, 38043 Grenoble Cedex, France*
(Received 10 December 1998)

We have performed optical reflectivity experiments and band structure diffraction calculations on fcc photonic crystals, consisting of air spheres in titania (TiO_2). The spectra reveal Bragg peaks whose large widths agree well with the calculations. The peaks overlap in many directions, causing the propagation of light to be limited by Bragg reflection to 45% of the 4π solid angle. This illustrates that the air-sphere crystals interact so strongly with light that an unprecedented limitation in the directions of propagation of light in photonic crystals is achieved.

PACS numbers: 42.70.Qs, 42.25.Fx, 81.05.Zx

Photonic crystals are three dimensionally periodic composites of dielectric materials, with lattice constants of the order of the wavelength of light [1,2]. Light that travels through such crystals experiences a periodic variation of the refractive index, analogous to the periodic potential energy of an electron in an atomic crystal [3]. Therefore, the dispersion relations of light in a photonic crystal can be expressed as photonic band structures in a Brillouin zone. The variation of the refractive index determines the strength of the interaction between light and a crystal. The interaction causes the splitting of degenerate bands and the appearance of frequency gaps for wave vectors at the edges of the Brillouin zone [3]. Waves with frequencies within these stop bands are Bragg reflected and cannot propagate. Stop bands are associated with every propagation direction. The widths of the stop bands increase with the interaction strength. If the interaction is very strong, the stop bands in all directions overlap to form a photonic band gap, that is, a frequency band for which the propagation of light is inhibited in all directions, 4π sr solid angle. Photonic band gaps are being vigorously pursued to control the spontaneous emission of excited atoms, or to localize light [1,2]: recently, a laser cavity made from a single defect in a two-dimensional photonic crystal has been demonstrated [4].

In this Letter, we analyze for the first time the optical band structure of strongly photonic crystals, consisting of air spheres in a solid with a high refractive index [5]. We have performed exhaustive reflectivity experiments, supported by new band structure diffraction calculations. It appears that the reflectivity measurements yield Bragg peaks of excellent quality that can be unambiguously interpreted, even for polycrystalline samples. The full widths at half maximum of the peaks agree well with the theoretically calculated widths of stop gaps. The air-sphere crystals reveal the widest Bragg peaks measured to date in photonic crystals. The Bragg peaks overlap over a wide range of angles, corresponding to stop bands already extending over 55% of the full solid angle. For comparison, colloidal photonic crystals or artificial opals exclude only about 8% of the full solid angle [6]. In other words, the air-sphere crystals interact so strongly with light that they impose a strong limitation on the directions in which light can propagate.

The photonic crystal samples consist of fcc crystals of air spheres in titania (TiO_2); see Ref. [5]. In brief, air-sphere crystals are made by filling the voids in artificial opals with a precursor of TiO_2 and then removing the opal by calcination (for related methods, see [7]). The fcc crystal structure, the radii of the air spheres, and the lattice constants were determined by synchrotron small-angle x-ray diffraction at the European Synchrotron Radiation Facility (ESRF), and by scanning electron microscopy. The average density of TiO_2 lies between 6 and 12 vol %, as determined by x-ray absorption. The samples either were contained inside flat glass capillaries or were freestanding. The samples have dimensions of a few mm and contain many crystal domains with typical sizes of $\sim 50\ \mu$m. The crystallites have flat faces normal to the [111] axis, as is apparent from scanning electron microscopy pictures. The other crystal axes are randomly oriented. The colorful optical Bragg reflections are easily seen with the unaided eye [5]. This is illustrated in Fig. 1, which shows a sample under white light illumination.

Figure 2 shows the setup for frequency and angle-resolved reflectivity experiments. The output of a broadband Philips UHP Hg lamp (25 W luminous power) is focused on a pinhole, which acts as a point source. The light is collimated and sent through a Fourier-transform interferometer (Biorad FTS-60A) operating with a spectral resolution of 16 cm^{-1}. The light beam is focused to a 0.6 mm diameter spot on the sample. The sample is mounted on a goniometer head to align the face of a crystal to the incident beam. The goniometer is centered on a rotation stage (α circle) (Fig. 2). The reflected light is collected with 10° angular resolution by a Si diode, which

 0031-9007/99/83(14)/2730(4)$15.00

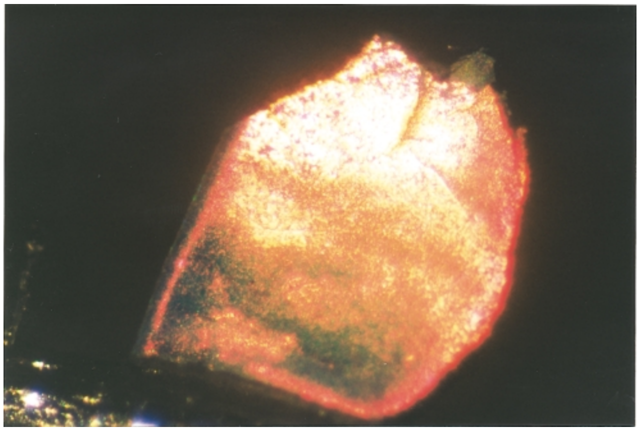

FIG. 1 (color). Photomicrograph of an air-sphere crystal (Sample No. 241-4). The sample is illuminated at normal incidence by a white light source. The sample measures 0.8 mm from left to right.

is mounted on an independently rotating stage that determines the scattering angle 2θ. The diode signal yields an interferogram that is Fourier transformed to get the spectrum of the reflected light. The spectra were referenced to those of a silver mirror with $>95\%$ reflectivity.

We have performed reflectivity experiments on many samples, having lattice constants a ranging from 340 to 620 nm. Here we concentrate on samples with $a \sim 480$ nm. Figure 3 shows specular reflectivity spectra ($\alpha + \theta = 90°$; see Fig. 2) as a function of frequency for several angles of incidence. Strong peaks are apparent, which are the result of constructive interference of waves reflected by consecutive 111 crystal planes. The peaks shift to higher frequencies with increasing angle of incidence, which confirms that the peaks result from Bragg diffraction [3,8]. Thus, in Fig. 3 the orientation of the incident and reflected wave vectors are scanned over the face of the Brillouin zone, and the stop gaps are tracked. The maximum reflectivity in Fig. 3 is as high as 20% at normal incidence. The maximum is less than 100% for several possible reasons: First, the incident beam illuminates many crystal domains, some of which may be misaligned and thus reflect nonspecularly. Second, light is scattered in all directions, hence mostly nonspecularly, by defects at the sample surface (cf. [5], Fig. 2). Only a few defects are apparent in the bulk of the crystals; hence the Bragg reflections of the crystals are strong and can be easily seen (Fig. 1) and detected. The maximum of the diffraction peaks in Fig. 3 decreases with increasing α, similar to angular effects in dielectric stacks [9]. There is a clear overlap between the reflection peak at normal incidence and the peak at the largest angle of incidence. This overlap indicates that there is a considerable overlap between the stop gaps in various directions in reciprocal space, signaling a strong interaction between light and the crystals.

Figure 4 shows the frequencies of the reflectivity maximum and the lower and upper half heights of each diffraction peak as a function of angle of incidence (black, red, and blue symbols, respectively). An excellent reproducibility between different measurements is apparent, and the estimated error bars on the data points are about 100 cm^{-1}. For the largest angles, only the lower reflection band edge could be discerned. The lower and upper edge frequencies increase with α deviating from normal incidence and largely follow the behavior of the maxima. It is well-known from the theory of x-ray diffraction that

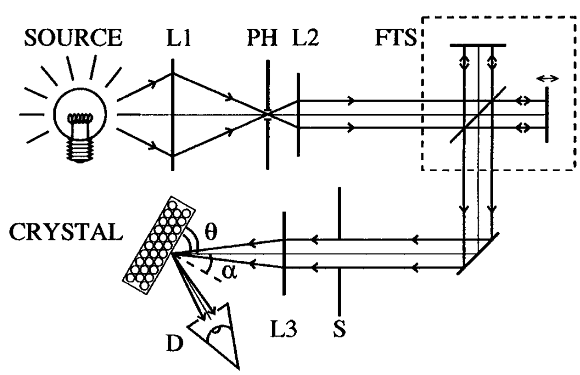

FIG. 2. Schematic drawing of the reflectivity setup. L1, L2, and L3 are lenses ($f_{L1} = 70$ mm, $f_{L2} = 25$ mm, and $f_{L3} = 70$ mm), PH is a pinhole (diameter $= 95$ μm), FTS is a Fourier-transform spectrometer, S is a stop (diameter $= 25$ mm), and D is the detector. α is the angle between the incident beam and the surface normal of the crystal and θ is the angle between the incident beam and the diffracting crystal planes.

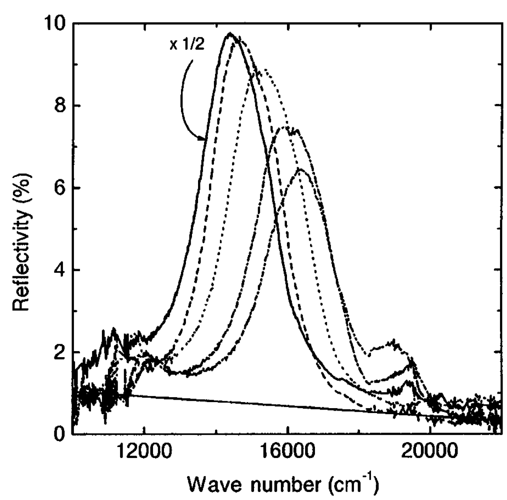

FIG. 3. Reflectivity of an air-sphere crystal (Sample No. 241-6, positioned on the top of a needle) as a function of frequency ($\omega/2\pi c$) in wave numbers. The solid curve, which has been scaled down by a factor of $1/2$, was obtained at normal incidence ($\alpha = 0°$). The other curves were obtained at external angles of incidence $\alpha = 15°$, $25°$, $35°$, and $40°$, in order of increasing frequency. The straight line is an estimate of the background for all spectra.

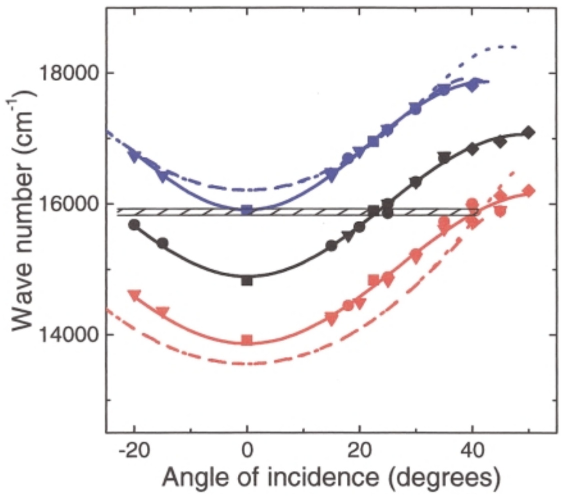

FIG. 4 (color). Frequencies of the reflectivity maxima (black data), and the upper (blue data) and lower (red data) half heights of the reflectivity as a function of the angle of incidence α (Sample No. 241-4). Different symbols distinguish data from different measurements. The solid curves are guides to the eye. The hatched bar indicates the wide angular range over which Bragg scattering takes place for frequencies at the top of the L gap ($\alpha = 0°$). Theoretical band structure diffraction calculations for $\epsilon = 6.25$ are indicated by the red dashed curve (lower edge, L-U trajectory), red dotted curve (lower edge, L-W trajectory), blue dashed curve (upper edge, L-U trajectory), and blue dotted curve (upper edge, L-W trajectory).

the width of a stop gap in the band structure maps on the readily observable width of the crystal's diffraction peak [8]. Perfect crystals have a diffraction peak with a flat top whose width is equal to that of a stop gap [8]. In addition to this intrinsic photonic width, extra broadening of the optical diffraction peaks may be caused in absence of extinction by finite crystal size and other imperfections. With a grain size of 50 μm (190 lattice spacings), finite size broadening is estimated as $1/190 = 0.5\%$, which is negligible. More important is the effect of extinction, e.g., by diffuse scattering, as the top becomes rounded, whereas the width remains unaffected [8]. Since the full width at half height (FWHM) of the optical diffraction Bragg peaks is a quantity that can be unambiguously determined, the use of this width to infer the width of stop bands is fully justified. The mapping between the widths of stop bands and the widths of frequency gaps in the band structure allows us to immediately associate the observed very broad reflection peaks of our air-sphere crystals with the occurrence of very broad frequency gaps in their band structure. The benchmark for photonicity, the amount of overlap occurring between various stop bands can be readily derived from Fig. 4: frequencies at the top of the stop band at $\alpha = 0°$ remain inside the region of half heights to angles of more than $\alpha = 40°$ (cf. bar in Fig. 4).

To corroborate our experimental data, we have performed calculations of the widths of stop bands using band structure diffraction calculations. The (111) diffraction requires an incoming wave vector $\mathbf{k}_{\rm in}$ and an outgoing diffracted wave vector $\mathbf{k}_{\rm out} = \mathbf{k}_{\rm in} + \mathbf{G}_{111}$, with $\mathbf{G}_{111}$ the 111 reciprocal lattice vector [3]. The wave vectors satisfy momentum conservation $|\mathbf{k}_{\rm in}| = |\mathbf{k}_{\rm out}|$, and energy conservation $E(\mathbf{k}_{\rm in}) = E(\mathbf{k}_{\rm out})$. Consequently, $\mathbf{k}_{\rm in}$ and $\mathbf{k}_{\rm out}$ are on the surface of the Brillouin zone (see Fig. 5). The band structure energies were calculated using the well-established plane wave methods [10,11]. This calculation identifies Bragg diffraction between propagating modes in the crystal on the edges of the stop gaps. The calculations were done for close-packed air spheres in dielectric with a dielectric constant ϵ ranging from 5.76 to 6.76, which is appropriate for TiO_2 [5]. It was checked that a total of 663 plane waves in the expansion gave a good relative convergence for the relevant lower bands and polarization effects were not included. The calculations yield the frequency of the diffracted light at the edge of a stop gap versus the diffraction angle inside the crystal. Frequency versus the diffraction angle outside the crystal (using Snell's law) are shown in Fig. 4 for $\mathbf{k}_{\rm in}$ along the representative L-U and the L-W trajectories in reciprocal space (dashed and dotted curves). It appears that the calculated frequencies are very close for both trajectories. This implies that the orientational average about the [111] axis that takes place in the experiment does not affect the center frequencies and widths of the Bragg reflections. The calculated widths of the stop gaps agree well with the FWHM widths of the Bragg reflections, which again justifies the identification of the widths of stop bands with the widths

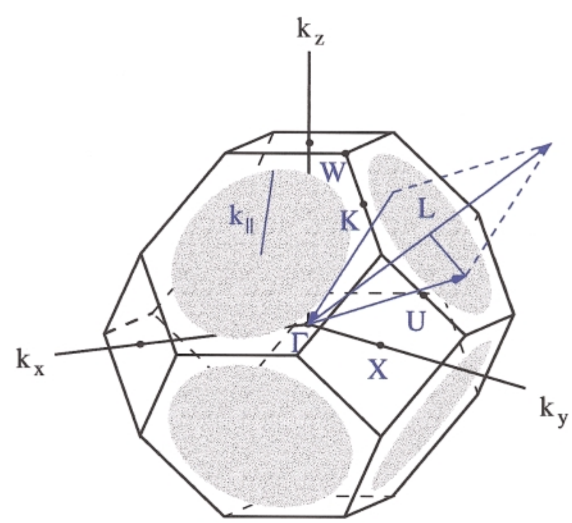

FIG. 5 (color). The first Brillouin zone of the fcc structure of the air-sphere crystals. Γ indicates the origin of reciprocal space, and K, L, U, and W are high symmetry points on the edge of the Brillouin zone. The arrow from the zone edge to Γ denotes the wave vector of an incident light beam, and the arrow from Γ to the zone edge indicates the wave vector of a reflected light beam. The long arrow from Γ through L is the 111 reciprocal lattice vector that is probed in the experiment. The shaded circles with radius $k_\parallel = k_{\rm L} \times 0.59$ indicate the range of wave vectors for which light with a frequency at the top of the L-stop band is reflected.

of Bragg peaks. This result agrees with previous experiments on weakly photonic opals and colloidal crystals, which revealed FWHM in excellent agreement with the width of the L gap obtained from normal band structure calculations [12].

The reflection data can be analyzed as a function of the wave vector inside the crystal, because the component of the wave vector parallel to the air-sample interface $\mathbf{k}_{\parallel}$ is conserved [13]. The length of $\mathbf{k}_{\parallel}$ is determined by the frequency ω in air and the angle of incidence α in air: $k_{\parallel} = |\mathbf{k}_{\parallel}| = \omega/c \sin\alpha$. Physically, $k_{\parallel}$ is the radius of a circle on the surface of the first Brillouin zone (cf. Fig. 5). We normalize $k_{\parallel}$ to the norm of the wave vector at the L point (normal incidence in Fig. 4), i.e., $k_{\mathrm{L}} = G_{111}/2$, which is obtained from the known lattice parameter. For frequencies at the top of the L gap, Bragg scattering takes place for wave vectors on the surface of the Brillouin zone with parallel components as large as $k_{\parallel}/k_{\mathrm{L}} = 0.59 \pm 0.02$ (see Fig. 5). The shaded circles centered around the L points illustrate that light of this frequency cannot enter the photonic crystals and, conversely, no light can be emitted from inside for this wide range of wave vectors. The excluded range of solid angle for each 111 Bragg reflection is $(0.28 \pm 0.02) \times \pi$ sr. Since there are eight of these reflections by symmetry, the total excluded range of solid angle is $(2.2 \pm 0.1) \times \pi$ sr, i.e., 55% of the full solid angle. This should lead to large changes in the important optical density of states, in particular, the local density of states [14]. A full photonic band gap might be anticipated if the Bragg reflection extends over the whole Brillouin zone, i.e., up to $k_{\parallel}/k_{\mathrm{L}} = 0.83$ (W point). It is known, however, that the fcc structure develops a band gap from higher than the first order stop bands [11].

Previously, evidence has been presented that the interpretation of transmission data may be complicated by the occurrence of so-called uncoupled modes [15]. These are Bloch modes in a photonic crystal that cannot be excited with external plane waves in perfect crystals with particular orientations for symmetry reasons. It is unlikely that such modes play a role in the present experiments, due to imperfections in crystal surfaces, finite angular resolution, and the averaging over crystal directions.

Information about the optical properties of photonic crystals can not only be obtained from reflection measurements, as we have shown here, but in principle also from transmission measurements. At frequencies beyond a stop band, however, the transmission is always strongly reduced due to diffuse scattering by inevitable defects [3,12]. This complication hampers the determination of stop band edges and becomes more severe with increasing relative refractive index variation. The excellent agreement between the widths of reflection peaks and calculated stop bands demonstrates that reflectivity experiments are superior to transmission experiments, in particular, in the physically interesting limit of a large relative refractive index variation.

We thank G. Derra and M. Schuurmans (Philips N.V.) for kindly providing the Hg lamp, and the staff of ESRF for help. This work is part of the research program of the "Stichting voor Fundamenteel Onderzoek der Materie" (FOM) and is made possible by financial support of the "Nederlandse Organisatie voor Wetenschappelijk Onderzoek" (NWO).

*Author for correspondence.
Electronic address: wvos@phys.uva.nl
URL:www.wins.uva.nl/research/scm

[1] E. Yablonovitch, Phys. Rev. Lett. **58**, 2059 (1987); S. John, *ibid.* **58**, 2486 (1987).
[2] *Photonic Band Gap Materials,* edited by C. M. Soukoulis (Kluwer, Dordrecht, 1996).
[3] N. W. Ashcroft and N. D. Mermin, *Solid State Physics* (Holt, Rinehart, and Winston, New York, 1976).
[4] O. Painter, R. K. Lee, A. Scherer, A. Yariv, J. D. O'Brien, P. D. Dapkus, and I. Kim, Science **284**, 1819 (1999).
[5] J. E. G. J. Wijnhoven and W. L. Vos, Science **281**, 802 (1998).
[6] M. Megens, J. E. G. J. Wijnhoven, A. Lagendijk, and W. L. Vos, Phys. Rev. A **59**, 4727 (1999).
[7] A. Imhof and D. J. Pine, Nature (London) **389**, 948 (1997); B. T. Holland, C. F. Blanford, and A. Stein, Science **281**, 538 (1998); A. A. Zakhidov *et al., ibid.* **281**, 897 (1998).
[8] R. W. James, *The Optical Principles of the Diffraction of X-Rays* (Bell, London, 1954).
[9] A. Yariv and P. Yeh, *Optical Waves in Crystals* (Wiley, New York, 1994), Chap. 6.
[10] K. M. Leung and Y. F. Liu, Phys. Rev. Lett. **65**, 2646 (1990); Z. Zhang and S. Satpathy, *ibid.* **65**, 2650 (1990); K. M. Ho, C. T. Chan, and C. M. Soukoulis, *ibid.* **65**, 3152 (1990).
[11] H. S. Sözüer, J. W. Haus, and R. Inguva, Phys. Rev. B **45**, 13 962 (1992); K. Busch and S. John, *ibid.* **58**, 3986 (1998).
[12] W. L. Vos *et al.,* J. Phys. Condens. Matter **8**, 9503 (1996); W. L. Vos, J. E. G. J. Wijnhoven, and M. Megens, *Conference on Lasers and Electro-Optics Europe* (IEEE/LEOS, Piscataway, NJ, 1998), p. 361; (to be published).
[13] M. Born and E. Wolf, *Principles of Optics* (Pergamon, Oxford, 1980).
[14] R. Sprik, B. A. van Tiggelen, and A. Lagendijk, Europhys. Lett. **35**, 265 (1996).
[15] W. M. Robertson *et al.,* Phys. Rev. Lett. **68**, 2023 (1992); K. Sakoda, Phys. Rev. B **55**, 15 345 (1997).